$\Omega_{\rm M}$ and Ω_Λ from 11 SNe Ia Observed with WFPC-2 on HST

R. A. Knop and the Supernova Cosmology Project

Version 2003-Feb-13

ABSTRACT

Type Ia Supernovae have provided the best direct evidence for dark energy. When combined with measurements of massive clusters and the Cosmic Microwave Background, those measurements provide a consistent picture of the universe as geometrically flat with a low mass density ($\Omega_{\rm M} \lesssim 0.3$); the greatest fraction ($\sim 70\%$) of the universe's energy density is in a cosmological constant or dark energy. This paper presents results on 11 supernovae with high-quality lightcurves measured with WFPC-2 on HST. The results from these new high-redshift supernovae yield cosmological results consistent with the previous SN Ia results. High precision measurements of the colors of the supernovae indicate that all but one of the new objects are not significantly affected by host galaxy dust extinction, but the precision of the measurements allow direct and individual E(B-V) corrections to be made separately for each object. Combining these data with the previous work of the Supernova Cosmology Project yield a measurement for a flat universe of $0.19^{+0.11}_{-0.07}$ (thus requiring a cosmological constant of $\Omega_\Lambda = 0.81$), slightly lower than earlier results but consistent to the $1-\sigma$ level. Under the assumption of a flat universe and combined with $\Omega_{\rm M}$ measurements from observations of the density of massive clusters., the combined data set provides a 68% upper confidence limit on w, the equation of state of the dark energy, of -0.8, consistent with the value $w = -1$ of a true cosmological constant.

1. Introduction

In 1998, two teams reported observations of Type Ia Supernovae (SNe Ia), which gave strong evidence for a non-zero cosmological constant, or dark energy density, and hence for the acceleration of the universe's expansion (Perlmutter *et al.* 1999; Riess 1998). These results ruled out to extremely high confidence a flat, matter-dominated universe; motivated by the prediction of a flat universe from inflation (REF??), they yielded a value for the cosmological constant of $\Omega_\Lambda \simeq 0.7$. Even

in the absence of assumptions about the geometry of the universe, the supernova results indicated greater than 99% confidence in the existence of a cosmological constant for plausible values of the mass density ($\Omega_{\rm M}$).

The supernova results combined with observations of the power spectrum of the Cosmic Microwave Background (CMB) (Jaffe *et al.* 2001, e.g.) and the density of massive clusters (Bahcall *et al.* 2003, e.g.) yield a consistent picture of a flat universe with $\Omega_{\rm M} \simeq 0.3$ and $\Omega_\Lambda \simeq 0.7$ (Bahcall *et al.* 1999). Each of these measurements are sensitive to different linear combinations of the parameters, and hence they complement each other. Moreover, because there are three different measurements of two parameters, the combination builds in an important consistency check. While the current observations of massive clusters and high-redshift supernovae primarily probe the "recent" universe at redshifts of $z < 1$, the CMB measurements probe the early universe at $z \sim 1100$. That consistent results are obtained by measurements of vastly different epochs of the universe's history is a vindication of the standard model of the expanding universe, and lend confidence that the cosmological parameters have been measured accurately.

Currently, the supernova results are sensitive to a linear combination of $\Omega_{\rm M}$ and Ω_Λ close to $\Omega_{\rm M} - \Omega_\Lambda$. As such, for a flat universe, of the three aforementioned cosmological measurements, taken alone the supernovae provide the best *direct* evidence for dark energy. Therefore, it is of importance both to improve the precision of the result, but also to confirm the result with additional independent high-redshift supernovae, and also to limit the possible effects of systematic errors.

This paper presents 11 new supernovae discovered and observed by the Supernova Cosmology Project (SCP) at redshifts $0.35 < z < 0.86$, a range very similar to that of the 42 high-z supernovae reported by this time in Perlmutter *et al.* (1999, hereafter P99). However, whereas the supernovae of that paper, with one exception, were observed entirely with ground-based telescopes, the 11 supernovae of this work have complete lightcurves in both the R and I bands measured with the Wide-Field/Planetary Camera (WFPC-2) on the Hubble Space Telescope (HST). The HST provides two primary advantages for photometry of point sources such as supernovae. First, from orbit, the sky background is much lower, allowing a much higher signal to noise ratio in a single exposure. Second, because the telescope is not limited by atmospheric seeing, it has very high spatial resolution. This helps the signal to noise ratio by greatly reducing the area of background emission which contributes to the noise of the source measurement, and moreover simplifies the task of separating the variable supernova signal from the host galaxy. With these advantages, the precision of the lightcurve measurements is so much greater for the 11 supernovae in this paper than was the case with the 42 SNe of P99 that even though there are only 1/4 as many objects, just these 11 high-redshift supernovae provide limits on the cosmological parameters comparable to the limits from the previous work. These 11 supernovae are the first new complete set of supernovae which confirm the accelerating universe results

since the original announcements in 1998.

One obvious possible systematic effect is the effect of host galaxy dust. For a given mass density, the effect of a cosmological constant on the magnitudes of high-redshift supernovae is to make their observed brightness *dimmer* than would have been the case with $\Omega_\Lambda = 0$. Similarly, dust extinction from within the host galaxy of the supernovae could have a similar effect. However, dust extinction will also tend to redden the colors of the supernovae. Therefore, a measurement of the color of the high-redshift supernovae, compared to the know colors of SNe Ia, can provide a upper limit on the effect of host galaxy dust extinction, or a direct measurement of that extinction which may then be corrected. P99 had R-I color measurements (corresponding to B-V measurements in the rest frame) for most of their 42 SNe; however, the uncertainties on *individual* color measurements were such that making host galaxy extinction corrections on each supernova was impractical. However, that paper presented evidence that the high-redshift sample as a whole was not effected by significant dust extinction compared to the low-redshift comparison sample of supernovae, and therefore its results may be viewed with confidence. The much higher precision of the HST lightcurves of this paper allow us to make high quality individual host galaxy extinction corrections to each supernovae event.

In this paper, we first describe the PSF-fit photometry method used for extracting the lightcurves from the WFPC-2 images. Next, we describe the lightcurve fitting procedure, including the methods used for calculating accurate K-corrections. So that all supernovae may be treated consistently, we apply the slightly updated K-correction procedure to all of the supernovae used in P99, and show that the new K-corrections do not change the results of that work. We discuss the evidence for host galaxy extinction (only significant for one of the 11 new supernovae) from the R-I lightcurve colors. We present the limits on the cosmological parameters $\Omega_{\rm M}$ and Ω_Λ from the new dataset alone as well as combining this data set with the data of P99; this latter fit provides the best current limit on cosmological parameters from high-redshift SNe Ia. Finally, we present the limits on w, the equation of state of the dark energy, from these data, and from these data combined with recent results from observations of the density of massive clusters.

2. Observations, Data Reduction, and Lightcurve Fits

2.1. WFPC2 Photometry

The supernovae discussed in this paper are listed in Table 1. They were discovered during three different supernova searches similar to those described in Perlmutter *et al.* (1999). Two of the searches were conducted at the 4m Blanco telescope at the Cerro Tololo Inter-American Observatory (CTIO), in December 1997 and March/April 1998. The final search was conducted at the Canada-France-Hawaii Telescope (CFHT) on Mauna Kea in Hawaii in April/May 2000. Each supernova was discovered in a two-epoch search. Images were acquired at two epochs separated by 3-4 weeks. Images from the first epoch were subtracted from images from

the second epoch; residual signals represented supernova candidates. Spectra obtained at the 10m Keck and 8m VLT observatories (and ESO 3.6m? check this) confirmed the identification of the candidates as SNe Ia, and measured the redshift of each candidate. Where possible, the redshift z of each candidate was measured by matching narrow features in the host galaxy of the supernovae; the precision of these measurements in z is typically 0.001. In cases where there were not sufficient host galaxy features, redshifts were measured from the supernova itself; in these cases, z is only precise to typically 0.01. However, even in the latter case redshift measurements are precise enough so as to be dwarfed by photometric errors.

Each of these supernovae was followed with two broadband filters with the Wide Field/Planetary Camera 2 (WFPC2) on the Hubble Space Telescope (HST). Table 1 lists the dates of these observations. The two filters were chosen to be those closest to the ground-based R-band (F675W) and I-band (F814W) filters. These filters correspond to redshifted B- and V-band filters for supernovae at $z < 0.7$, and redshifted U- and B- band filters for supernovae at $z > 0.7$. Each listed observation comprises at least two images taken within the same orbit, split for purposes of cosmic ray rejection. In some cases (the longer exposures), a single observation is the sum of more than two images.

The HST images were reduced through the standard HST data reduction pipeline (ACONLEY– HELP ME OUT HERE, ANYTHING MORE TO SAY?). Photometric fluxes were extracted from the final images using a PSF-fitting procedure. Traditional PSF fitting procedures assume a single isolated point source above a constant background. In this case, the point source was superimposed on top of the image of the host galaxy. In all cases, the supernova image was separated from the core of the host galaxy; however, in most cases the separation was not enough that an annular measurement of the background would be accurate. Because the host galaxy flux should be constant in all of the images, we used a PSF fitting procedure which fit a PSF *simultaneously* to every image of a given supernovae observed through a given photometric filter. The model we fit was:

$$f_i(x,y) = f_{0i} * \mathrm{psf}(x - x_{0i}, y - y_{0i}) + \mathrm{bg}(x - x_{0i}, y - y_{0i}; a_j) + z_i \quad (1)$$

where $f_i(x,y)$ is the measured flux in pixel (x,y) of the ith image, f_{0i} is the total flux in the supernova in the ith image, $\mathrm{psf}(u,v)$ is a normalized point spread function, $\mathrm{bg}(u,v)$ is a constant background parametrized by a_j, and z_i is a pedestal offset for the ith image. There are $4n+m-1$ parameters in this model, where n is the number of images (typically 2, 5, or 6 summed images) and m is the number of parameters a_j that specifies the background model (typically 3 or 6). The -1 is due to the fact that a zeroth-order term in the background is degenerate with one of the z_i terms. The model was fit to 7×7 or 9×9 patches extracted from all of the images of a time sequence of a single candidate in a single filter.

A single Tiny Tim PSF, corrected by an empirical electron diffusion term Fruchter

Table 1: WFPC2 Supernova Observations

SN Name	z	F675W Observations	F814W Observations
1997ek	0.863	1998-01-05 (800s)	1998-01-05 (1200s)
		1998-01-11 (800s)	1998-01-11 (1200s)
			1998-02-02 (2300s)
			1998-02-14 (2300s)
			1998-02-27 (2300s)
			1998-11-09 (2400s)
			1998-11-16 (2400s)
1997eq	0.538	1998-01-06 (600s)	1998-01-06 (600s)
		1998-01-21 (800s)	1998-01-11 (1200s)
			1998-02-02 (1200s)
		1998-02-11 (800s)	1998-02-11 (1200s)
		1998-02-19 (800s)	1998-02-19 (1200s)
1997ez	0.778	1998-01-05 (800s)	1998-01-05 (1200s)
		1998-01-11 (800s)	1998-01-11 (1200s)
			1998-02-02 (2300s)
			1998-02-14 (2300s)
			1998-02-27 (4600s)
9878	0.644	1998-04-08 (600s)	1998-04-08 (600s)
		1998-04-19 (600s)	1998-04-19 (600s)
		1998-04-30 (800s)	1998-04-30 (1200s)
		1998-05-15 (800s)	1998-05-15 (1200s)
		1998-05-28 (800s)	1998-05-28 (1200s)
1998as	0.355	1998-04-08 (800s)	1998-04-08 (1200s)
		1998-04-20 (800s)	1998-04-20 (1200s)
		1998-05-11 (800s)	1998-05-11 (1200s)
		1998-05-15 (800s)	1998-05-15 (1200s)
		1998-05-29 (800s)	1998-05-29 (1200s)
1998aw	0.440	1998-04-08 (600s)	1998-04-08 (600s)
		1998-04-18 (600s)	1998-04-18 (600s)
		1998-04-29 (800s)	1998-04-29 (1200s)
		1998-05-14 (800s)	1998-05-14 (1200s)
		1998-05-28 (800s)	1998-05-28 (1200s)
1998ax	0.497	1998-04-08 (600s)	1998-04-08 (600s)
		1998-04-18 (600s)	1998-04-18 (600s)
		1998-04-29 (800s)	1998-04-29 (1200s)
		1998-05-14 (800s)	1998-05-14 (1200s)
		1998-05-27 (800s)	1998-05-27 (1200s)
1998ay	0.638	1998-04-08 (800s)	1998-04-08 (1200s)
		1998-04-20 (800s)	1998-04-20 (1200s)
			1998-05-11 (2300s)
			1998-05-15 (2300s)
			1998-06-03 (2300s)
1998ba	0.430	1998-04-08 (600s)	1998-04-08 (600s)
		1998-04-19 (600s)	1998-04-19 (600s)
		1998-04-29 (800s)	1998-04-29 (1200s)
		1998-05-13 (800s)	1998-05-13 (1200s)
		1998-05-28 (800s)	1998-05-28 (1200s)
1998bi	0.740	1998-04-06 (800s)	1998-04-06 (1200s)
		1998-04-18 (800s)	1998-04-18 (1200s)
			1998-04-28 (2300s)
			1998-05-12 (2300s)
			1998-06-02 (2300s)
2000fr	0.543		2000-05-08 (2200s)
		2000-05-15 (1200s)	2000-05-15 (1200s)
		2000-05-28 (1200s)	2000-05-28 (1200s)
		2000-06-10 (1000s)	2000-06-10 (800s)
		2000-06-22 (2400s)	2000-06-22 (2300s)
		2000-07-08 (2400s)	2000-07-08 (2300s)

(2000), was used for all images of a given band. Although this is an approximation– the PSF of WFPC2 depends on the epoch of the observation as well as the position on the chip– this approximation should be a good one. All of the supernovae were positioned close to the center of the chip. To verify that this approximation was valid, we reran the PSF fitting procedure with individually generated PSFs for most supernovae; the measured fluxes were not significantly different.

Fluxes extracted in this manner were corrected for the charge transfer efficiency (CTE) of WFPC-2 following the procedure of Dolphin (2000) (updated by the coefficients posted later on the author's web page– how do I cite this?). Because the galaxy background is a smooth background underneath the point source, it was considered as a contribution to the background in the CTE correction. For an image which was a combination of several separate exposures within the same orbit or orbits, the CTE calculation was performed assuming that each image had a measured flux whose fraction of the total flux was equal to the fraction of that individual image's exposure time to the summed image's total exposure time.

Ground-based photometric fluxes were extracted from images using the same aperture photometry procedure of P99. A complete lightcurve in a given filter (R or I) combined the HST data with the ground-based data, using measured zeropoints for the ground based data and the Vega zeropoints of Dolphin (2000) for the HST data. An uncertainty of 0.02 was assumed for all HST zeropoints; this uncertainty was added as a correlated error between all HST data points when combining with the ground-based lightcurve. Similarly, the measured uncertainty in the ground-based zeropoint was added as a correlated error to all ground-based fluxes.

2.2. Lightcurve Fits

In order to perform lightcurve first, data from WFPC2 was combined with additional data obtained at ground-based observatories. Photometry from the following telescopes contributed to the 11 SNe in Table 1: the CTIO 4m and the CFHT 3.6m (telescopes used in the search), the INT 2.6m telescope, then WIYN 3.5M telescope, and the Keck 10m telescope.

In addition to the 11SNe described here, lightcurve fits were also performed to the supernovae from P99 (including 18 supernovae from Hamuy *et al.* (1996, hereafter H96)), and nine from Riess (1999, hereafter R99) which match the same selection criteria used for the H96 supernovae (must have data within 6 days of maximum light; must be in the Hubble Flow, i.e. at $z > xxx$). Because of new templates and K-corrections (see below), the lightcurve fits from P99 were redone for this paper, although exactly the same photometry was used.

Lightcurve fits were performed using a chi-square minimization procedure based on MINUT (REF?). Fits were performed to template lightcurves, and were performed simultaneously to the R and I band data for high-redshift supernovae. (The exception is the seven high-redshift supernovae from P99 for which no I-band lightcurve is available.) For low-redshift supernovae, so as to match as closely as possible the data fit for high redshift su-

pernovae, fits were performed using only the B and V band data (which correspond to de-redshift R and I bands for most of the high-redshift supernovae). The lightcurve model fit to the supernova had four parameters to modify the lightcurve templates: time of rest-B maximum of the lightcurve, peak flux in R, R-I color, and stretch s. Stretch (Goldhaber *et al.* 2001) is a parameter which multiplies the time axis of the lightcurve template, so that a supernova with a high stretch has a relatively slow decay from maximum, and a supernova with a low stretch has a relatively fast decay from maximum. For supernovae in the redshift range $z = 0.3$–0.7, a B template was fit to the R-band lightcurve and a V template was fit to the I-band lightcurve. For the three supernovae at $z > 0.7$, a U template was fit to the R-band lightcurve and a B template to the I-band lightcurve.

The B template used in the lightcurve fits was that of Goldhaber *et al.* (2001). For this paper, new V-band and R-band templates were generated following a procedure similar to that of Goldhaber *et al.* (2001), by fitting a smooth parametrized curve through the low-z supernova data of H96 and R99. A new U-band template was generated with data from Hamuy *et al.* (1991), Lira *et al.* (1998), Richmond *et al.* (1995), Suntzeff *et al.* (1999), and Wells *et al.* (1994). Each of these new templates was fit to the low-redshift supernova data simultaneously with a stretch fit of the B-template to the B-band data of the same supernova, thereby guaranteeing that the fit templates correspond to a $s = 1$ supernova. Lightcurve templates had an initial parabola with an 20-day rise time (Aldering *et al.* 2000), joined to a smooth spline section to describe the main part of the lightcurve, then joined to an exponential decay to describe the final tail at $>\sim 70$ days past maximum light. The first 90 days of each of the three templates is shown in Table 2. Note that due a secondary "hump" or "shoulder" xx days after maximum, the R-band lightcurve does not appear to vary strictly according to the single simple stretch parameter which is so successful in describing the different B- and V-band lightcurves. Nonetheless, the lightcurve fits performed in this paper assume that the R-band template is adequately described by stretch. The effects of this on any results of this paper will be small, as the R-band template was only used for two of the supernovae, both from P99: 1997I at $z = 0.172$ and 1997N at $= -0.180$.

For most of the supernovae, the zero offset of the lightcurve was fixed at zero, and not varied as a parameter. For the high-redshift supernovae, this is consistent with the assumption that the galaxy has been properly subtracted from each photometric data point, an assumption made implicitly when combining data integrated in different apertures (due to varying seeing conditions, or, in the extreme case, due to the very small PSF of WFPC2). For seven low-redshift supernovae, the zero offsets of the B and V-band lightcurves were allowed to vary as parameters, as the addition of these parameters produced substantial (factor of 2-3) improvements in the chi-square of the fit. The supernovae treated in this fashion were 1992ag, 1992bo, 1992bp, 1993B, 1995ak, 1996ab, and 1996bo. Additionally, for six high-redshift supernovae (1997J, 1997O, 1997Q, 1997R, 1997K, and

Table 2: U, V, and R Lightcurve Templates Used

Day[1]	U flux[2]	V flux[2]	R flux[2]	Day[1]	U flux[2]	V flux[2]	R flux[2]
-19	6.712e-03	4.960e-03	5.779e-03	31	4.790e-02	2.627e-01	3.437e-01
-18	2.685e-02	1.984e-02	2.312e-02	32	4.524e-02	2.481e-01	3.238e-01
-17	6.041e-02	4.464e-02	5.201e-02	33	4.300e-02	2.345e-01	3.054e-01
-16	1.074e-01	7.935e-02	9.246e-02	34	4.112e-02	2.218e-01	2.887e-01
-15	1.678e-01	1.240e-01	1.445e-01	35	3.956e-02	2.099e-01	2.733e-01
-14	2.416e-01	1.785e-01	2.080e-01	36	3.827e-02	1.990e-01	2.592e-01
-13	3.289e-01	2.430e-01	2.832e-01	37	3.722e-02	1.891e-01	2.463e-01
-12	4.296e-01	3.174e-01	3.698e-01	38	3.636e-02	1.802e-01	2.345e-01
-11	5.437e-01	4.017e-01	4.681e-01	39	3.565e-02	1.721e-01	2.237e-01
-10	6.712e-01	4.960e-01	5.779e-01	40	3.506e-02	1.649e-01	2.137e-01
-9	7.486e-01	5.889e-01	6.500e-01	41	3.456e-02	1.583e-01	2.046e-01
-8	8.151e-01	6.726e-01	7.148e-01	42	3.410e-02	1.524e-01	1.962e-01
-7	8.711e-01	7.469e-01	7.725e-01	43	3.365e-02	1.471e-01	1.884e-01
-6	9.168e-01	8.115e-01	8.236e-01	44	3.318e-02	1.423e-01	1.813e-01
-5	9.524e-01	8.660e-01	8.681e-01	45	3.266e-02	1.378e-01	1.747e-01
-4	9.781e-01	9.103e-01	9.062e-01	46	3.205e-02	1.337e-01	1.687e-01
-3	9.940e-01	9.449e-01	9.382e-01	47	3.139e-02	1.299e-01	1.630e-01
-2	1.000e+00	9.706e-01	9.639e-01	48	3.072e-02	1.263e-01	1.578e-01
-1	9.960e-01	9.880e-01	9.834e-01	49	3.005e-02	1.229e-01	1.529e-01
0	9.817e-01	9.976e-01	9.957e-01	50	2.945e-02	1.195e-01	1.483e-01
1	9.569e-01	1.000e+00	1.000e+00	51	2.893e-02	1.161e-01	1.440e-01
2	9.213e-01	9.958e-01	9.952e-01	52	2.853e-02	1.128e-01	1.398e-01
3	8.742e-01	9.856e-01	9.803e-01	53	2.830e-02	1.096e-01	1.359e-01
4	8.172e-01	9.702e-01	9.545e-01	54	2.827e-02	1.064e-01	1.320e-01
5	7.575e-01	9.502e-01	9.196e-01	55	2.849e-02	1.033e-01	1.282e-01
6	6.974e-01	9.263e-01	8.778e-01	56	2.793e-02	1.003e-01	1.244e-01
7	6.375e-01	8.991e-01	8.313e-01	57	2.738e-02	9.743e-02	1.207e-01
8	5.783e-01	8.691e-01	7.821e-01	58	2.684e-02	9.467e-02	1.170e-01
9	5.205e-01	8.369e-01	7.324e-01	59	2.630e-02	9.207e-02	1.133e-01
10	4.646e-01	8.031e-01	6.842e-01	60	2.578e-02	8.964e-02	1.097e-01
11	4.113e-01	7.683e-01	6.396e-01	61	2.527e-02	8.741e-02	1.061e-01
12	3.610e-01	7.330e-01	6.007e-01	62	2.477e-02	8.538e-02	1.026e-01
13	3.145e-01	6.977e-01	5.691e-01	63	2.428e-02	8.359e-02	9.910e-02
14	2.725e-01	6.629e-01	5.444e-01	64	2.380e-02	8.207e-02	9.568e-02
15	2.356e-01	6.293e-01	5.254e-01	65	2.333e-02	8.083e-02	9.232e-02
16	2.044e-01	5.972e-01	5.113e-01	66	2.287e-02	7.927e-02	8.902e-02
17	1.783e-01	5.667e-01	5.011e-01	67	2.242e-02	7.774e-02	8.579e-02
18	1.567e-01	5.376e-01	4.938e-01	68	2.197e-02	7.624e-02	8.264e-02
19	1.388e-01	5.099e-01	4.887e-01	69	2.154e-02	7.476e-02	7.958e-02
20	1.239e-01	4.835e-01	4.848e-01	70	2.111e-02	7.332e-02	7.660e-02
21	1.115e-01	4.583e-01	4.814e-01	71	2.070e-02	7.191e-02	7.373e-02
22	1.008e-01	4.342e-01	4.776e-01	72	2.029e-02	7.052e-02	7.096e-02
23	9.144e-02	4.113e-01	4.725e-01	73	1.989e-02	6.916e-02	6.832e-02
24	8.314e-02	3.894e-01	4.653e-01	74	1.949e-02	6.782e-02	6.581e-02
25	7.583e-02	3.685e-01	4.552e-01	75	1.911e-02	6.651e-02	6.344e-02
26	6.941e-02	3.486e-01	4.414e-01	76	1.873e-02	6.523e-02	6.199e-02
27	6.380e-02	3.296e-01	4.247e-01	77	1.836e-02	6.397e-02	6.057e-02
28	5.891e-02	3.115e-01	4.058e-01	78	1.799e-02	6.274e-02	5.918e-02
29	5.467e-02	2.943e-01	3.855e-01	79	1.764e-02	6.153e-02	5.783e-02
30	5.102e-02	2.781e-01	3.645e-01	80	1.729e-02	6.034e-02	5.650e-02

1: Day is relative to the epoch of the maximum of the B-band lightcurve.
2: Relative fluxes.

1997am) the I-band zero-offset was allowed to vary as a parameter, due to the lack of a supernova-free host galaxy image for those supernovae given the lightcurve data used in P99.

The final results of the lightcurve fits, including the effect of color corrections and K-corrections (and the host galaxy E(B-V) dust extinctions measured as part of that process) are listed in Table 3 for the 11 supernovae of this paper. Table 4 shows the results of lightcurve fits for the 42 high-redshift supernovae of P99, and Table 5 shows the results of lightcurve fits for the low-redshift supernovae from H96 and R99.

2.3. Color- and K-Corrections

In order to combine data from different telescopes, it is necessary to perform color corrections to remove the differences in the spectral responses of the filters. For the ground based telescopes, the filters are close enough to the standard Bessel filter (Bessell 1990) that a single linear color term (measured at each observatory with standard stars) suffices to put the data onto the Bessel system. The WFPC2 filters are enough different from the ground-based filters, however, that a linear term is not sufficient, and moreover the differences between a SN Ia and standard star spectral energy distribution (SED) are significant. In this case, color corrections were calculated by integrating template SN Ia spectra, described below.

In order to perform lightcurve template fitting, a K-correction (Nugent *et al.* 2002) must be applied to transform the data in the observed filter into a rest-frame magnitude in the filter used for the lightcurve template. The color correction to the nearest standard Bessel filter followed by a K-correction to a rest-frame filter is equivalent to a direct K-correction from the observed filter to the standard rest-frame filter. In practice, we perform the two steps separately so that all photometry may be combined to provide a lightcurve effectively observed through a standard (e.g.) R-band filter, which may then be K-corrected and fit with a single series of K-corrections.

Color and K-corrections were performed following the procedure of Nugent *et al.* (2002). In order to perform these corrections, a template SN Ia spectrum described in that paper is necessary. The template used in this paper began with the template of that paper, but then had a smooth multiplicative function applied to the template at each day so that integration of the spectrum through the standard filters would produce the proper intrinsic colors for a Type Ia supernova, including a mild dependence of those intrinsic colors on stretch.

The intrinsic colors of the supernova were determined in the BVRI spectra range by smooth fits to the low-redshift supernovae of H96 and R99. For each color B-V, V-R, and R-I, every data point from those papers was K-corrected and corrected for Milky Way extinction. These data were plotted together, and then a "ridge-line" fit of a smooth curve (parametrized by a spline under tension) was fit to the plot of color versus date relative to maximum. Two curves were fit, an "intercept" curve $b(t)$ and a "slope" curve $m(t)$, so that at any given date the intrinsic color was

$$col = b(t') + m(t') \times 1/s \qquad (2)$$

Table 3: Supernova Lightcurve Fits: HST Supernovae from this paper

SN	z	m_X[1]	m_B[2]	Stretch	R-I[3]	E(B-V)$^4_{\rm MW}$	E(B-V)$^5_{\rm host}$	Notes
sn97198	0.538	22.65	23.23±0.03	0.99±0.03	0.15±0.03	0.044	-0.04±0.05	
sn97201	0.863	23.39	24.58±0.03	1.05±0.01	0.83±0.07	0.042	-0.13±0.12	
sn97226	0.778	23.27	24.39±0.04	1.06±0.04	0.70±0.06	0.026	0.08±0.12	
sn9819	0.430	22.34	22.95±0.05	0.92±0.02	0.06±0.04	0.024	-0.02±0.05	
sn9855	0.440	22.64	23.29±0.02	1.02±0.02	0.29±0.03	0.026	0.23±0.04	6
sn9878	0.644	23.31	23.89±0.04	0.76±0.03	0.41±0.06	0.029	0.07±0.08	
sn98104	0.638	23.28	23.91±0.08	1.05±0.05	0.25±0.07	0.035	-0.10±0.10	
sn98109	0.497	22.59	23.20±0.05	1.10±0.03	0.12±0.05	0.035	0.00±0.06	
sn98122	0.355	22.20	22.71±0.03	0.94±0.02	0.17±0.03	0.037	0.08±0.05	
sn98142	0.740	22.95	24.00±0.03	0.95±0.04	0.53±0.05	0.026	0.00±0.10	
C00-008	0.543	22.52	23.14±0.03	1.08±0.01	0.10±0.03	0.030	-0.08±0.05	

1: X=R for $z < 0.7$, X=I for $z > 0.7$. (ROB CHECK THIS)

2: This value has been K-corrected and corrected for Milky Way E(B-V) extinction, but not for host galaxy extinction. Measurement uncertainties include only the uncertainties from the photometry, not including the zeropoint uncertainty (which is correlated between the supernovae, and put into the cosmological fits separately).

3: This is just the measurement uncertainty, and does not include any intrinsic color dispersion.

4: Schlegel *et al.* (1998)

5: This is the observed R-I color at the epoch the rest-frame B-band lightcurve peak. This includes an intrinsic color dispersion of 0.03 for $z < 0.7$ (where R-I maps to rest-frame B-V), and 0.08 for $z > 0.7$ (where R-I maps to rest-frame U-B).

6: Omitted from Fits 1–3. (Section 3.2, Table 8)

Table 4: Supernova Lightcurve Fits: New Fits to Perlmutter (1999) SNe

SN	z	m_X[1]	m_B[2]	Stretch	R-I[3]	E(B-V)$^4_{\rm MW}$	E(B-V)$^5_{\rm host}$	Notes
sn921	0.458	22.13	22.80±0.08	0.86±0.45	—	0.010	—	7
sn94102	0.420	22.37	22.48±0.05	1.04±0.15	—	0.136	—	7
sn94191	0.374	21.32	21.79±0.03	0.89±0.03	—	0.031	—	6, 7
sn94264	0.378	22.13	22.47±0.07	1.02±0.12	—	0.066	—	7
sn94281	0.372	21.81	22.28±0.04	0.89±0.04	—	0.031	—	7
sn94361	0.354	22.06	22.50±0.14	0.69±0.14	—	0.036	—	7
sn94351	0.425	21.68	22.36±0.05	0.87±0.01	0.18±0.13	0.008	0.11±0.15	
sn9568	0.400	21.79	22.28±0.03	1.19±0.04	-0.12±0.10	0.040	-0.16±0.11	
sn9569	0.498	23.02	23.68±0.06	1.04±0.09	0.15±0.20	0.021	0.03±0.22	
sn9570	0.453	22.60	23.24±0.06	0.87±0.10	0.02±0.13	0.022	-0.09±0.14	
sn9579	0.465	22.69	23.37±0.06	0.88±0.10	0.43±0.22	0.022	0.34±0.24	
sn95103	0.450	22.46	22.66±0.07	0.97±0.07	0.08±0.14	0.181	-0.12±0.15	
sn95104	0.480	22.64	23.05±0.04	0.88±0.06	0.21±0.16	0.114	0.02±0.18	
sn95110	0.388	22.08	22.64±0.05	0.97±0.05	0.01±0.10	0.018	-0.05±0.11	
sn95116	0.655	22.61	23.25±0.03	1.05±0.06	0.34±0.11	0.019	-0.01±0.14	
sn95126	0.615	22.54	23.20±0.06	1.13±0.07	0.13±0.21	0.033	-0.19±0.26	
sn962	0.570	22.70	23.30±0.03	1.00±0.05	0.16±0.08	0.040	-0.06±0.10	
sn963	0.490	22.46	23.09±0.03	1.01±0.04	0.35±0.06	0.035	0.24±0.08	6
sn969	0.495	22.19	22.82±0.02	0.97±0.04	0.08±0.07	0.028	-0.05±0.08	
sn9617	0.656	23.09	23.76±0.05	0.89±0.08	0.19±0.26	0.032	-0.22±0.33	
sn9621	0.828	23.35	24.51±0.15	0.96±0.23	0.57±0.18	0.035	-0.34±0.26	
sn9624	0.450	22.67	23.26±0.07	0.90±0.06	0.25±0.16	0.049	0.14±0.18	
sn9626	0.430	22.58	23.25±0.03	0.89±0.07	0.38±0.08	0.025	0.32±0.10	6
sn970	0.172	20.16	20.44±0.01	0.96±0.01	0.10±0.02	0.051	0.13±0.04	
sn971	0.526	22.69	23.24±0.03	0.89±0.05	0.31±0.17	0.051	0.14±0.20	
sn972	0.763	23.48	24.41±0.39	0.82±0.09	0.09±0.44	0.043	-0.71±0.60	
sn974	0.580	22.89	23.48±0.06	1.05±0.07	0.25±0.20	0.040	0.02±0.24	
sn975	0.619	23.20	23.83±0.06	1.03±0.11	0.19±0.32	0.039	-0.13±0.40	
sn976	0.550	22.89	23.49±0.05	0.94±0.06	—	0.025	—	7
sn9710	0.180	20.39	20.59±0.01	1.07±0.02	-0.01±0.03	0.031	0.02±0.05	
sn9733	0.374	22.99	23.53±0.08	1.05±0.09	0.09±0.16	0.029	0.04±0.17	6, 7
sn9738	0.472	22.52	23.16±0.04	0.88±0.04	0.26±0.14	0.033	0.14±0.16	
sn9739	0.612	23.04	23.77±0.04	1.21±0.07	-0.08±0.24	0.033	-0.43±0.29	
sn9742	0.430	22.01	22.61±0.02	0.94±0.02	0.07±0.14	0.030	-0.01±0.15	
sn9748	0.592	23.73	24.38±0.10	1.09±0.15	0.24±0.34	0.020	0.01±0.41	
sn9760	0.657	23.28	23.88±0.05	0.98±0.06	0.35±0.18	0.030	-0.01±0.24	
sn9765	0.320	21.43	21.90±0.01	1.06±0.02	0.08±0.04	0.027	0.02±0.06	
sn9779	0.450	22.33	22.93±0.03	0.76±0.07	0.21±0.08	0.045	0.07±0.10	
sn9781	0.579	22.91	23.58±0.07	0.86±0.05	0.02±0.23	0.028	-0.25±0.28	
sn9784	0.830	23.17	24.35±0.07	1.00±0.06	0.92±0.09	0.026	0.18±0.15	
sn9785	0.416	21.91	22.45±0.05	1.04±0.06	-0.06±0.10	0.036	-0.13±0.11	
sn9794	0.581	22.85	23.48±0.04	1.50±0.07	0.14±0.15	0.033	-0.08±0.18	

1: X=R for $z < 0.7$, X=I for $z > 0.7$ (ROB CHECK THIS)
2: As in Table 3
3: As in Table 3
4: Schlegel *et al.* (1998)
5: As in Table 3
6: Omitted from Fits 1–3 (Section 3.2, Table 8)

Table 5: Supernova Lightcurve Fits: Low-z SNe from Hamuy (1996) and Riess (1999)

SN	z	m_B[1]	Stretch	B-V[2]	$E(B-V)^3_{MW}$	$E(B-V)^4_{host}$	Notes
1990O	0.030	16.15±0.02	1.14±0.02	0.05±0.02	0.10	0.00±0.04	
1990af	0.051	17.76±0.01	0.76±0.01	0.07±0.01	0.04	0.00±0.03	
1992P	0.025	16.08±0.01	1.02±0.01	0.00±0.02	0.02	0.02±0.03	
1992ae	0.075	18.41±0.04	0.96±0.02	0.09±0.03	0.04	-0.02±0.04	
1992ag	0.025	16.14±0.04	1.16±0.03	0.14±0.03	0.10	0.10±0.04	
1992al	0.015	14.48±0.01	0.96±0.01	0.03±0.01	0.04	-0.02±0.03	
1992aq	0.102	19.29±0.05	0.89±0.03	0.09±0.03	0.01	-0.07±0.05	
1992bc	0.020	15.11±0.01	1.07±0.01	0.10±0.01	0.02	-0.07±0.03	
1992bg	0.035	16.67±0.02	1.01±0.01	0.17±0.02	0.18	0.01±0.03	
1992bh	0.045	17.58±0.02	1.03±0.02	0.10±0.02	0.02	0.08±0.04	
1992bl	0.044	17.34±0.02	0.81±0.01	0.04±0.02	0.01	0.01±0.04	
1992bo	0.019	15.75±0.01	0.74±0.01	0.00±0.02	0.03	-0.02±0.03	5
1992bp	0.079	18.25±0.02	0.92±0.02	0.03±0.02	0.07	-0.12±0.04	
1992br	0.088	19.31±0.08	0.71±0.02	0.14±0.05	0.03	0.00±0.06	5
1992bs	0.064	18.22±0.03	1.03±0.01	0.01±0.02	0.01	-0.04±0.04	
1993B	0.070	18.35±0.08	0.98±0.04	0.10±0.04	0.08	-0.03±0.06	
1993O	0.051	17.64±0.01	0.95±0.01	0.05±0.01	0.05	-0.02±0.03	
1993ag	0.049	17.80±0.02	0.95±0.01	0.22±0.02	0.11	0.10±0.04	
1994M	0.023	16.28±0.02	0.86±0.01	0.07±0.02	0.02	0.08±0.04	
1994S	0.015	14.77±0.02	1.05±0.02	0.07±0.02	0.02	-0.04±0.04	
1995E	0.012	16.68±0.02	1.03±0.02	0.73±0.02	0.03	0.77±0.04	5
1995ac	0.050	17.04±0.01	1.11±0.01	0.02±0.01	0.04	-0.03±0.03	
1995bd	0.016	15.21±0.01	1.12±0.01	0.73±0.01	0.49	0.30±0.03	5
1996C	0.030	16.56±0.01	1.12±0.01	0.00±0.01	0.01	0.03±0.03	
1996ab	0.124	19.48±0.09	1.01±0.06	0.17±0.08	0.03	-0.08±0.10	
1996bl	0.036	16.64±0.01	1.03±0.01	0.09±0.01	0.10	0.02±0.03	
1996bo	0.017	15.90±0.01	0.86±0.01	0.50±0.01	0.08	0.46±0.03	5

1: Measurement uncertainties as for note 2 in Table 3.

2: This is the measured B-V color at the epoch of rest-frame B-band lightcurve maximum.

3: Schlegel *et al.* (1998)

4: Includes an assumed intrinsic B-V color dispersion of 0.03 magnitudes.

5: These SNe were omitted from all cosmology fits (Section 3.2).

where $t' = t/(s(1+z))$, z is the redshift of the supernova, and s is the stretch of the supernova from a simultaneous fit to the B and V lightcurves (matching the procedure used for most of the high redshift supernovae). No host galaxy extinction corrections were applied to the data. Instead, host galaxy extinction was handled by fitting the blue side ridge-line of the supernova color curves, so as to extract the unreddened intrinsic color. This ridge-line fit was performed by adding an asymmetric intrinsic error bar (longer to the red than to the blue), and by omitting supernovae from the fit which were systematically reddened relative to the median value.

Some of our data extends into the U-band range of the spectrum. This is obvious for supernovae at $z > 0.7$ where a U-band template is fit to the R-band data. However, even for supernovae at $z \gtrsim 0.55$, the de-redshifted R-band filter begins to overlap the U-band range of the rest-frame spectrum. Thus, it is also important to know the intrinsic U-B color so as to generate a proper spectral template. We used data from the literature in Table 6. Here, there is an insufficient number of supernova lightcurves to reasonably use the sort of ridge-line analysis used above to eliminate the effects of host galaxy extinction in determining the intrinsic BVRI colors. Instead, for U-B, we perform extinction corrections using the E(B-V) values from Phillips *et al.* (1999), so as to measure an intrinsic U-B color that is likely to be right. It is clear that more U-B data on low redshift supernovae is necessary in order to determine the true intrinsic U-B color of a SN Ia, and the dispersion in that intrinsic color. (For example, 1994D is a well-known as an otherwise normal SN Ia which is over-luminous in the ultraviolet.) Based on the table, we assumed a U-B color of -0.4 at the epoch of rest-B maximum, with a dispersion of 0.08 magnitudes (used for error calculations in cosmological fits). Note that this is 0.2 magnitudes bluer than the color implicitly assumed by P99; the effect of this difference will be discussed in Section 3.1.

Once a template spectrum with the proper intrinsic colors has been produced for each day relative to the date of B maximum, it is necessary to further modify it for each supernova to reflect dust extinction in the supernova host galaxy, and extinction of the redshifted spectrum due to the Milky Way. Reddening effects from dust were calculated given the E(B-V) parameter (measured from the lightcurve fits for the host galaxy, and given by Schlegel *et al.* (1998) for the Milky Way) and the extinction law of O'Donnell (1994).

For each supernova, this finally modified spectral template was integrated through the Bessel and WFPC2 filter transmission functions to provide color and K-corrections. Note that the exact spectral template needed for a given data point on a given supernova is dependent on parameters of the fit: the stretch, the time of each point relative to the epoch of rest-B maximum, and the host galaxy E(B-V) (measured from the peak color of the lightcurve). Thus, color and K-corrections were performed iteratively with lightcurve fitting. An initial date of maximum, stretch, and host galaxy extinction was assumed. Those were used to color and K-correct the data, which was fit to the template. The parameters resulting from

Table 6: U-B SN Ia Colors

SN	Raw U-B[1]	Corrected U-B[2]	Reference
1980N	-0.21	-0.29	Hamuy *et al.* (1991)
1989B	0.08	-0.33	Wells *et al.* (1994)
1990N	-0.35	-0.45	Lira *et al.* (1998)
1994D	-0.50	-0.52	Wu *et al.* (1995)
1998bu	-0.23	-0.51	Suntzeff *et al.* (1999)

1: This is the measured U-B value from the paper

2: This is U-B K-corrected, and corrected for host galaxy and Milky Way extinction

that fit were used to generate new color and K-corrections, and the whole procedure was repeated until the results of the fit converged.

The E(B-V) values quoted in Tables 3, 4, and 5 are the necessary parameters for the extinction law of O'Donnell (1994) to reproduce the observed R-I color at the epoch of the maximum of the rest-frame B lightcurve. This reproduction was done by modifying the spectral template exactly as described above, given the intrinsic color of the supernova of the fit stretch, the Milky Way extinction, and the host galaxy E(B-V) parameter. The modified spectrum was integrated through the Bessel R and I band filters, and E(B-V) was varied until the R-I value produced matched the result from the lightcurve fit. (These E(B-V) values where then used to generate the proper color and K-corrections for the next iteration of each lightcurve fit.)

3. Results and Discussion

3.1. Colors and Extinction

Because new color and K-corrections have been applied to the data of P99, it is important to verify that the cosmological conclusions of that paper are not changed by those differences. Figure 3.1 shows the confidence limits on the cosmological parameters Ω_M and Ω_Λ (see Section 3.2) from P99 and with the exact same set of supernovae (the "Case C" subset from that paper), only with new lightcurve fits using the color and K-corrections, and template lightcurves, of this paper. Although the confidence intervals are slightly different, obviously the effect of these changes are small, and would not effect any of the conclusions of P99. Clearly, the details of the K-corrections are not a likely source of significant systematic error in the conclusions of P99 and Riess (1998).

The greatest improvement the data on the 11 WFPC2-observed supernovae in this paper shows over the previous high-redshift supernova data is that the R-I colors have been measured to much higher precision than was the case with the earlier data. In P99, extinction was estimated by comparing the mean host galaxy E(B-V) values from the low and high redshift samples. Although the uncertainties on individual E(B-V) values for high redshift supernovae were large, the uncertainty on the mean of the distribution was much

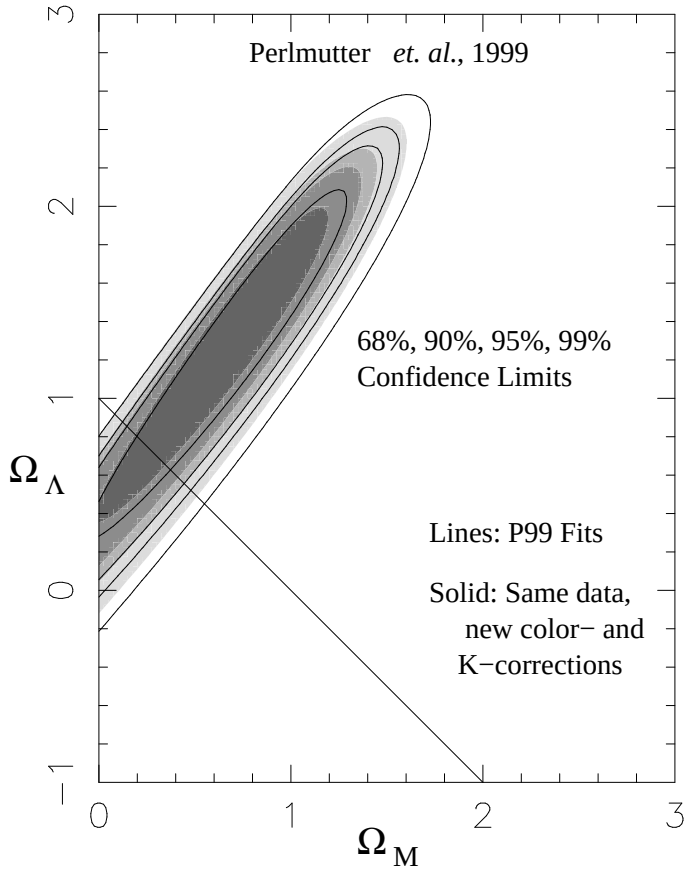

Fig. 1.— The effect of new color- and K-corrections on the Ω_M and Ω_Λ confidence limits from the "Case C" fits of P99. The lines are the confidence limits on Ω_M and Ω_Λ from that paper. The solid regions are confidence intervals which use exactly the same ground based supernova lightcurve data, but with the updated color- and K-corrections of this paper applied, as discussed in Section 2.3, and with the HST photometry of 1997ap re-measured using the procedure of Section 2.1

smaller. From this, P99 argued that, omitting two obviously reddened supernovae to create their "case C" subset, the high redshift supernovae did not show significant host galaxy reddening relative to the low redshift supernovae. Although they did not individually correct supernova distance moduli directly for host galaxy extinction, this argument provided confidence that the cosmological results were not strongly affected by such extinction.

Figure 2 shows histograms of the host galaxy E(B-V) values from different subsets of supernovae. For the lower three panels, overplotted is a line that shows the distribution of the H96 SNe (upper panel) given the E(B-V) uncertainties of each set. In other words, the line shows the distribution that would have been measured given the H96 E(B-V) values as a parent distribution, dispersed by the error bars (assumed Gaussian) of each other set. Visually, each set's distribution is consistent with the E(B-V) distribution from H96, except for H99 which shows several significantly reddened supernovae, and for the 11 HST SNe in this paper, one of which is significantly reddened. Table 7 lists the variance weighted mean E(B-V) values for each set. The "Fit 3" supernovae are equivalent

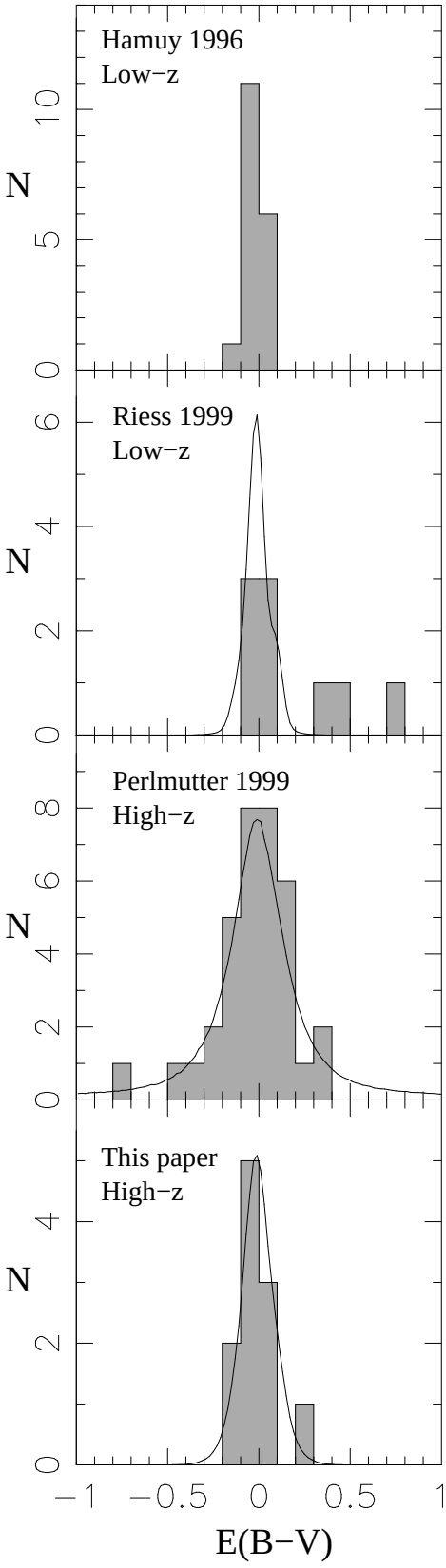

Fig. 2.— Histograms of E(B-V) for the four sets of supernovae used in this paper. All supernovae with measured colors (i.e. excluding seven from P99) are plotted. The solid lines drawn over the lower three panels is a simulation of the distribution expected if the H96 set represented the true distribution of SN colors, given the error bars of each set.

Table 7: Mean E(B-V) Values

Set	All SNe	Fit 3 SNe[1]
H96	-0.010 ± 0.009	-0.005 ± 0.009
R99	$+0.188 \pm 0.012$	$+0.008 \pm 0.015$
P99	$+0.048 \pm 0.019$	$+0.023 \pm 0.020$
This Paper	$+0.034 \pm 0.018$	-0.009 ± 0.020

1: SNe omitted from Fits 1-3 (Section 3.2, Table 8) have been omitted from these means. This includes outliers, as well as supernovae with E(B-V)$> 3\sigma$.

to "Case C" from P99. (The cosmological fits performed are discussed in Section 3.2.) The most severe outliers have been omitted as have supernovae which are significantly red. The "Fit 3" value for P99 includes 32 of the 42 SNe presented in that paper; seven have no color measurement, two are omitted because they are too red, and one is omitted as an outlet. The variance weighted mean E(B-V) for this set is 0.023 ± 0.020, which is only $\sim 1.3\sigma$ different from the mean of the H96 set, reaffirming the conclusion of P99 that this subset of SNe did not suffer significant host galaxy reddening on the average.

For the 11 HST supernovae in this paper, if 1998ba is omitted, then then mean E(B-V) of the set is consistent with the mean E(B-V) of both low redshift sets (where supernovae with E(B-V)¿3σ have been omitted from the R99 set). Even though strongly reddened supernovae have been omitted from each set to reach this conclusion, the conclusion is not circular. The uncertainty on individual E(B-V) values for the HST supernovae reported in this paper is typically 0.04–0.1 in addition to an assumed intrinsic dispersion of 0.03 (for supernovae where R-I maps to B-V) or 0.08 (for supernovae where R-I maps to U-B). Thus, only supernovae which are grossly reddened compared to the uncertainty *on the mean* have been omitted. It would be possible for there to still be a detectable *average* color excess among the remaining supernovae, even after the most grossly reddened supernovae have been omitted. Figure 2 and Table 7 argue that for the HST supernovae of this paper, the "Fit 3" subset does not have such an excess, and that the excess in the P99 supernovae compared to the low-redshift is E(B-V)$\lesssim$ 0.02–0.04. (Note, however, that the improved R-I color measurements on the high-redshift supernovae reported in this paper allow us to *individually* correct for E(B-V) extinction, as discussed in Section 3.2.)

One of the biggest differences that arises from intrinsic U-B color which is 0.2 magnitudes bluer than the one assumed in P99 (as discussed in Section 2.2) is apparent in Figure 2. In P99, a few of the higher redshift supernovae had large *negative* E(B-V) values (e.g., see Figure 6 in that paper). Whereas modest ($\lesssim 1\sigma$) negative E(B-V) values are expected for a distribution of supernovae which show no or only mild host galaxy extinction, multiple large negative values are a sign of a systematic problem, which in this case was a "too red" assumption about the intrinsic U-B color of a Type Ia supernova. The problem was exacerbated by the greater effect of extinction on the U-band, leading to even larger values of E(B-V) estimated from a bad E(U-B) determination. This effect was strongest for the supernovae at $z > 0.7$, where the

R-band data was fit to a U-band template. However, even supernovae at $z \gtrsim 0.5$ have some rest-frame U-band "contamination" in the observed R-band photometry.

3.2. Cosmological Parameters $\Omega_{\rm M}$ and Ω_Λ

Figure 3 shows Hubble Diagrams which plot both the new lightcurve fits to the data from P99, H96, and R99, as well as the new data on 11 SNe presented in this paper. For supernovae at $z > 0.7$, the peak rest-frame B magnitude was estimated from the peak of the I-band lightcurve. For supernovae at lower redshifts, it was estimated from the peak of the R-band lightcurve. In the lower panel of Figure 3, the filled points represent the new SNe from this paper; the improved error bars resulting from the WFPC2 lightcurves are apparent. Indeed, for many of the new supernovae, the error bars are dominated by the assumed 0.17 magnitude intrinsic dispersion of the peak-B magnitude of a SN Ia (REF?). The points fall along a distribution consistent with that of P99, and inconsistent with a Friedman model omitting Ω_Λ.

Figure 4 shows Hubble Diagrams where extinction corrections have been applied to the points. Here, the advantage of the WFPC2 data is even more apparent, although the distributions are consistent with the same cosmological models as is the case in Figure 3, where no extinction correction has been applied. In Figure 4, error bars have been expanded by $R_B \times E(B-V)$, where the O'Donnell (1994) extinction law and the spectral template discussed in Section 2.3 give $R_B = 4.34$ for a Type Ia supernova at $z = 0$ (the redshift of the supernova relative to the host galaxy where the extinction occurs). In addition to the measured error on R-I, an dispersion of 0.03 magnitudes was assumed on the intrinsic B-V color, and a dispersion of 0.08 magnitudes on the intrinsic U-B color. After host galaxy extinction corrections have been applied, the peak B magnitude is assumed to have an intrinsic dispersion of 0.12 magnitudes (REF).

Cosmological fits to the luminosity distance modulus equation from the Friedmann-Robertson-Walker metric followed the procedure of P99. The $\Omega_{\rm M}/\Omega_\Lambda$ plane was divided into a grid, and at each grid point a chi-square value was calculated by fitting the luminosity distance equation to the peak B-band magnitudes and redshifts of the supernovae. The range of parameter space explored was $\Omega_{\rm M} = (0$–$3)$, $\Omega_\Lambda = -1$–$3)$. Other than the implicit prior that $\Omega_{\rm M} > 0$, no further constraints were placed on the parameters; this parameter space was large enough to more than encompass 99% confidence intervals for any fit performed. In addition to $\Omega_{\rm M}$ and Ω_Λ, there were the same two "nuisance" parameters used in the fits of P99 which were integrated out in order to provide final $\Omega_{\rm M}/\Omega_\Lambda$ confidence limits. The first of these parameters is $\mathcal{M}$, which contains the combined effect of the Hubble constant (H_0) and the absolute magnitude of a SN Ia. (This fitting procedure does not require independent knowledge of either H_0 or the absolute SN Ia magnitude, and produces $\mathcal{M}$ as a measurement of the combined effect of both.) The second was α, the slope of the magnitude/stretch relationship. The peak magnitude of a SN Ia is mildly dependent on the lightcurve decay

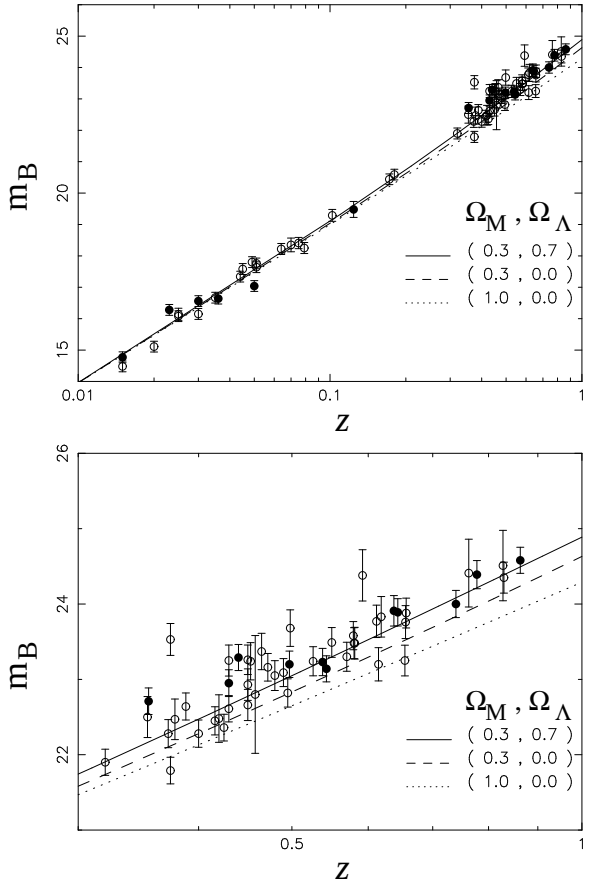

Fig. 3.— Hubble Diagram of effective m_B vs. redshift. Plotted at $z < 0.15$ are the 16 supernovae from H96 (open circles) and the 6 supernovae from R99 (filled circles) used in the cosmological fits. At $z > 0.15$, open circles are the 42 high-redshift supernovae from P99 and filled circles are the 11 supernovae of this work. K-corrections and Milky Way extinction corrections have been applied, but host galaxy extinction corrections have not been applied. Error bars include an 0.17 magnitude intrinsic dispersion. Lines represent luminosity distance modulus values calculated with the indicated parameters from the FRW metric, using a value of $\mathcal{M}$=-3.44 (the most probable value from our fits).

time scale, such that SNe with a slower decay (higher stretch) tend to be over-luminous, while SNe with a faster decay (lower stretch) tend to be under-luminous. This is parametrized by

$$m_{bcor} = m_b + \alpha(s-1). \qquad (3)$$

After the chi-square is calculated at each grid point, a probability is calculated according to $P \propto exp(-\chi^2/2)$; the probability of the whole 4-dimensional grid is normalized, and then integrated over the two axes corresponding to the "nuisance" parameters.

Supernovae were divided into two subsets, one for fitting without explicit extinction corrections, and one for fitting with explicit extinction corrections. The first set mimics the "Case C" subset of P99. That subset omitted six supernovae from that paper: 1992bo and 1992br, because they were outliers in the stretch distribution ($s < 0.75$); 1994H and 1997O, because they had the largest residuals from the fit; and 1996cg and 1996cn, because they showed evidence for substantial host galaxy extinction ($E(B-V) > 3\sigma$). We follow P99 and omit these six supernovae from our non-extinction-corrected fit. In addition, from the R99 supernovae, we omit three supernovae which show a very large amount of reddening: 1995E, 1995bd,

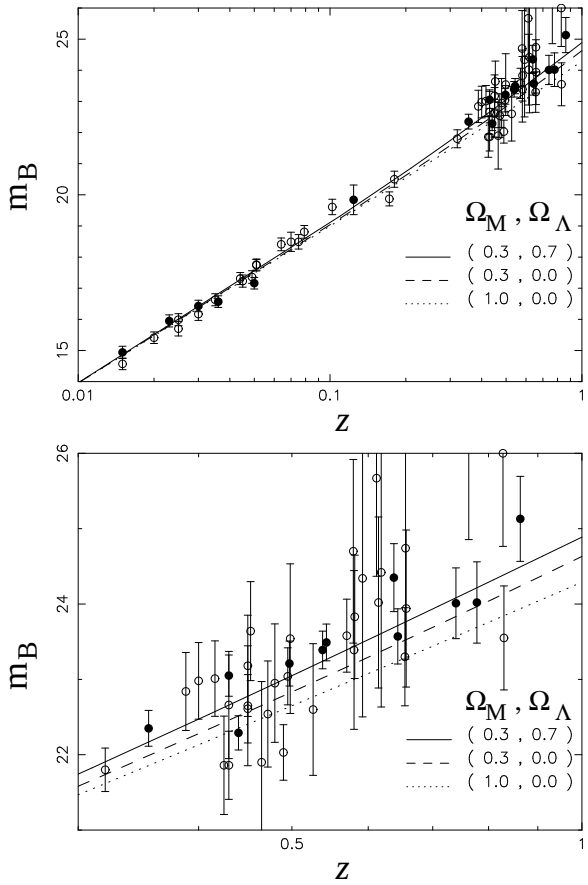

Fig. 4.— Hubble Diagram of effective m_B vs. redshift, similar to Figure 3. In this plot, host galaxy extinction corrections have been applied, adding to the measurement error an assumed intrinsic color dispersion of 0.03 magnitudes in B-V and 0.08 magnitudes in U-B. The intrinsic peak magnitude dispersion used in this plot is 0.12 magnitudes.

and 1996bo. (Note that 1995bd suffers a substantial quantity of Galactic extinction, with $E(B-V)_{MW} = 0.49$.) From the high-redshift supernovae in this paper, we omit 1998aw due to reddening.

For fits which include explicit reddening corrections, we allow 1994H, 1997O, and 1998aw back into the subset, as extinction will be explicitly handled. However, the three extremely reddened SNe from R99 show the three largest residuals from the fit, even when reddening corrections have been applied. Thus, they remain omitted from the reddening corrected subset.

In addition to uncertainties on the peak B-magnitude from the lightcurve fits, additional uncertainties contributed to the determination of each supernova's contribution to the chi-square. These included the uncertainty on the stretch, leveraged by an assumed $\alpha = 1.74$ (REF) (used for purposes of uncertainty only); a peculiar velocity error on the redshift of 300 km s^{-1}, folded into the magnitude error; and an intrinsic supernova dispersion of 0.17 (for fits without extinction corrections applied) or 0.12 (for fits with extinction correction applied) (REF). All points were corrected for Milky Way extinction using E(B-V) values from Schlegel *et al.* (1998); this correction was assumed to be uncertain to 10% of its value. Finally, only for the

fits which explicitly included host galaxy extinction corrections, we used the uncertainty on color correction, corresponding to $R_B = 4.35$ times the uncertainty on the $E(B-V)$ value plus an intrinsic color dispersion of 0.03 (for supernovae with B-V colors) or 0.08 (for supernovae with U-B colors).

The fits performed are summarized in Table 8, and plotted in Figures 5 and 6. Figure 5 shows the confidence intervals on $\Omega_{\rm M}$ and Ω_Λ for fits which do not explicitly correction for host galaxy extinction, but which omit substantially reddened supernovae. The solid confidence ellipses in the left panel includes the low-redshift supernovae plus ten high-redshift supernovae from this paper. The right panel adds the high-redshift supernovae from P99. For comparison, the confidence intervals using all of the low-redshift SNe, just the high-redshift SNe from P99 are drawn in dotted lines. (Removing the six additional supernovae from R99 has only a small effect on the confidence intervals.) Note that the ten supernovae in the left panel of Figure 5 represent a new, independent set of high-redshift supernovae, which confirm the accelerating universe results of 1998 (Riess 1998, P99,). This is the first full set of high redshift supernovae which provide comparable confidence limits since the original announcement of those two groups. Two features are important. First, the size of the confidence intervals from the 10 supernovae in this paper are comparable to the confidence intervals from the 38 high-redshift supernovae of P99; this is a result of the greater quality of the lightcurves measured here with WFPC2 on HST. Second, although the confidence intervals are not identical, they are consistent: the overlap of the inner, 68% confidence interval is analogous to the overlap of a 1-σ error bar. In particular, the conclusions of P99 are confirmed, that $\Omega_\Lambda > 0$ to $> 99\%$ confidence, and that the $\Omega_{\rm M} = 1, \Omega_\Lambda = 0$ universe is extremely inconsistent with the data. The solid confidence intervals in the right panel of Figure 5 combine the data from both high-redshift sets, and represent the SCP's current best limits on $\Omega_{\rm M}$ and Ω_Λ.

Figure 6 shows the fits when extinction corrections have been applied. Again, the left panel includes all of the low-redshift supernovae, but only the 11 high-redshift supernovae from this paper, while the right panel adds in 34 high-redshift supernovae from P99 (omitting the two omitted from the previous fit because they were the greatest outliers, and omitting an additional six SNe for which no R-I color measurement is available). On both panels, plotted in dotted lines, are the confidence intervals using just the high-redshift supernovae used in P99, as in Figure 5. Here, the improvement in the confidence intervals from the new high redshift data is dramatic, a direct result of the much better individual R-I color measurements available with the WFPC2 lightcurves.

The Hubble Diagrams of Figures 3 demonstrate that the data show high-redshift supernovae which are *dimmer* at a given redshift than would have been expected in a flat, $\Omega_{\rm M} = 1$ universe, leading to the conclusion that $\Omega_\Lambda > 1$. If the supernovae at higher redshifts were subject, on the average, to more host galaxy dust extinction than the supernovae at low redshifts, this could simulate the effect: the

Table 8: Cosmological fits performed

Fit #	Ext. Corr?	Sets Included	Number of Supernovae[1]	Min. χ^2	Ω_M for Flat[2]	Notes
1	No	H96 R99 P99	60	79	$0.25^{+0.08}_{-0.07}$	High-z SNe from P99
2	No	H96 R99 This paper	32	42	$0.20^{+0.08}_{-0.06}$	Only new high-z SNe
3	No	H96 R99 P99 This paper	70	92	$0.24^{+0.07}_{-0.06}$	All high-z SNe
4	Yes	H96 R99 P99	56	49	$0.30^{+0.17}_{-0.11}$	Fit 1 w/ extinction correction.
5	Yes	H96 R99 This paper	33	25	$0.12^{+0.10}_{-0.08}$	Fit 2 w/ extinction correction.
6	Yes	H96 R99 P99 This paper	67	63	$0.19^{+0.11}_{-0.07}$	Fit 3 w/ extinction correction.

1: All fits omitted two low-z supernovae with anomalously low stretches, and three low-z plus two high-z supernovae which were the greatest outliers. Fits 1-3 omitted supernovae with E(B-V) values $> 3\sigma$. Fits 4-6 omitted supernovae with no color measurement.

2: This is the intersection of the fit probability distribution with the the line that assumes $\Omega_M + \Omega_\Lambda = 1$.

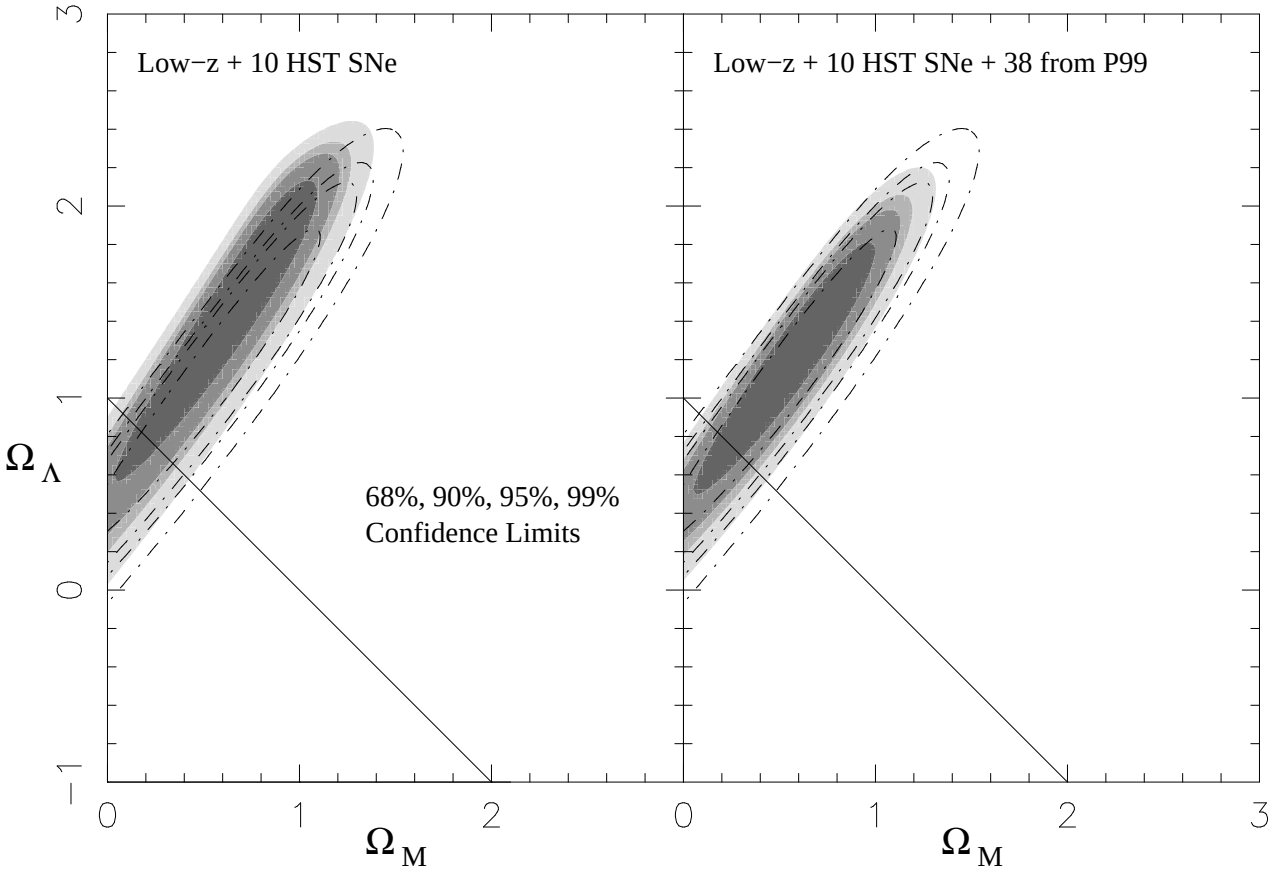

Fig. 5.— Joint confidence intervals on Ω_M and Ω_Λ using the data from this paper. Filled contours indicate the 68confidence intervals from each fit. For comparison, the new fits to just the data from P99 are plotted in dashed lines on each panel. Host galaxy extinction corrections have not been explicitly applied to the data that went into these fits. Left: The 22 low-z supernovae plus the 10 HST-observed supernovae of this paper (excluding 1998aw). Right: The 22 low-z supernovae, plus the 10 HST-observed supernovae of this paper, plus 38 high-z supernovae from P99.

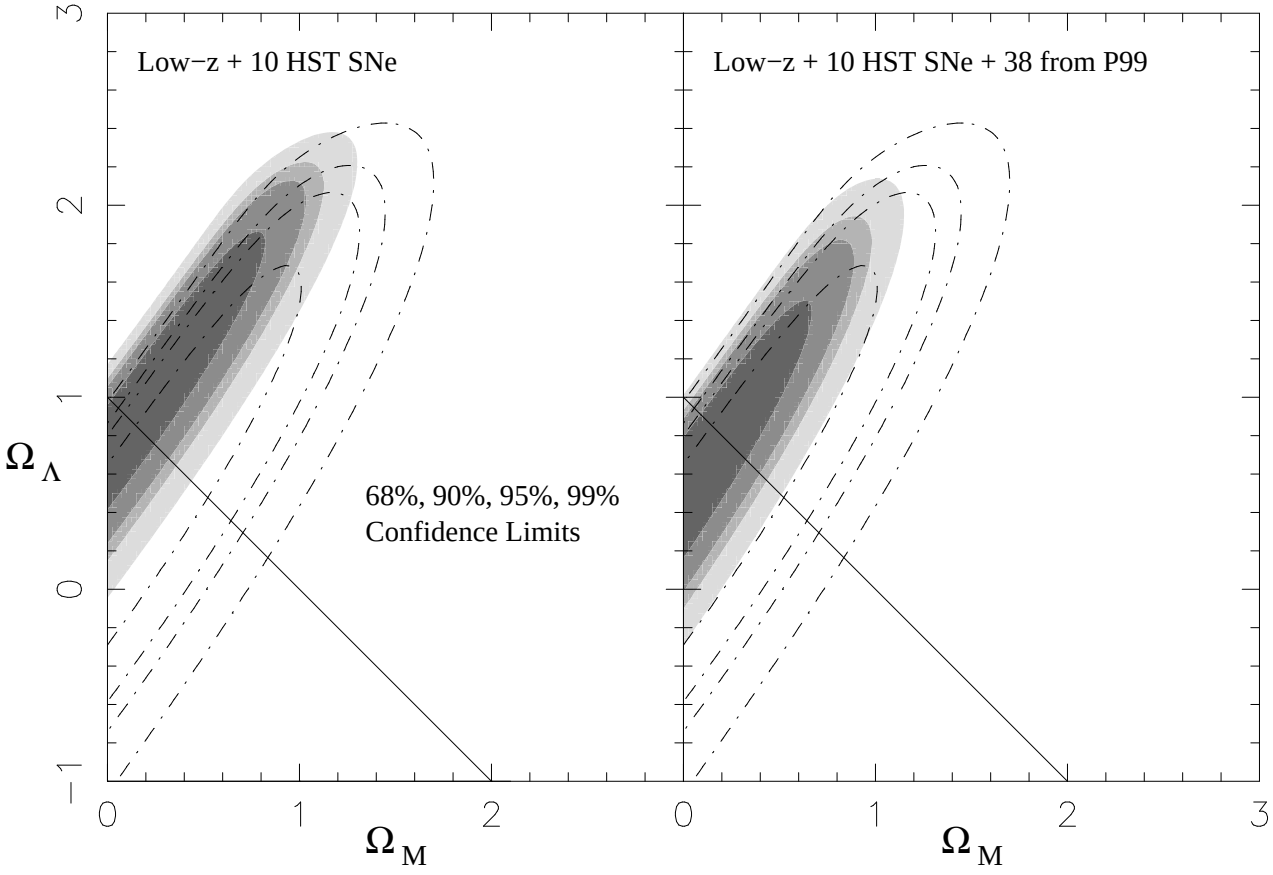

Fig. 6.— Joint confidence intervals on Ω_M and Ω_Λ using the data from this paper. Filled contours indicate the 68confidence intervals from each fit. For comparison, the new fits to just the data from P99 are plotted in dashed lines on each panel. For all of these fits, host galaxy extinction corrections based on measured E(B-V) values have been applied. Left: The 22 low-z supernovae plus the 11 HST-observed supernovae of this paper. Right: The 22 low-z supernovae, plus the 11 HST-observed supernovae of this paper, plus 34 high-z supernovae from P99.

higher redshifts supernovae would be systematically dimmer. However, because dust extinction effects bluer light more than redder light, its effects would show up in the colors of the supernovae. Criticisms of the 1998 conclusions that $\Omega_\Lambda > 1$ have included the worry that host galaxy extinction could have been more significant than was argued in those papers. As discussed in Section 3, there is evidence even for the P99 supernovae that the high redshift set is not, on average, more reddened than the low redshift set. That evidence is stronger for 10 of the 11 high redshift supernovae in this set, where more precise R-I measurements allow individual host galaxy extinction corrections for each supernova. Moreover, Figure 7, which shows our two primary confidence regions (fits 3 and 6 from Table 8, including all supernovae with and without host galaxy extinction corrections), shows that the dominant effect of applying host galaxy extinction corrections is *not* to move the confidence intervals closer to a flat, $\Omega_{\rm M} = 1$ universe, but rather to move the confidence ellipses toward lower mass, primarily along the major axis of the ellipse— although the difference is not very significant, as the most probable value for the fit without extinction corrections is within the 90% (or $2-\sigma$) confidence ellipse of the fit that includes extinction corrections.

The fits with extinction corrections applied confirm and strengthen the conclusions of P99: the high-redshift supernova data are inconsistent with a flat, $\Omega_{\rm M} = 1$ universe, and require $\Omega_\Lambda > 0$ to $> 99\%$ confidence. Under the assumption of flatness, the combined data favor a universe with $(\Omega_{\rm M}, \Omega_\Lambda) = (0.2, 0.8)$, although they agree with the $(\Omega_{\rm M}, \Omega_\Lambda) = (0.3, 0.7)$ universe of P99 to the $1-\sigma$ level.

4. Comparisons with Other Cosmological Measurements

In the last few years, a "consensus cosmology" has arisen combining three measurements (Bahcall *et al.* 1999): Type Ia supernova, the Cosmic Microwave Background (CMB), and the number density of clusters. This consensus cosmology is a flat, low mass universe with $(\Omega_{\rm M}, \Omega_\Lambda) \simeq (0.3, 0.7)$. Measurements of the angular power spectrum of the CMB yields a maximum likelihood value of $\Omega_{\rm M} + \Omega_\Lambda = 1.2$, but are consistent with the flat universe value of $\Omega_{\rm M} + \Omega_\Lambda = 1.0$ (Jaffe *et al.* 2001). The mass function of clusters, meanwhile, indicates that the mass density of the universe is low, $\Omega_{\rm M} \leq 0.3$ (Bahcall *et al.* 2003). Together, these results are consistent with the requirement from the data reported in this paper that $\Omega_{\rm M} > 0$, even for a low density universe.

As is clear from Figure 7, our results are more sensitive to a combination close to $\Omega_{\rm M} - \Omega_\Lambda$ than to either variable independently. This nicely complements the CMB measurements, which are more sensitive to $\Omega_{\rm M} + \Omega_\Lambda$, and the cluster measurements, which are sensitive primarily to $\Omega_{\rm M}$ (although that is convolved with sensitivity to σ_8). The sensitivity of these three methods to different linear combinations of the parameters is what Bahcall *et al.* (1999) term the "Cosmic Triangle". Because there are only two parameters, whereas there are three measurements, even though the methods complement each other, there is enough information that it is significant that the confi-

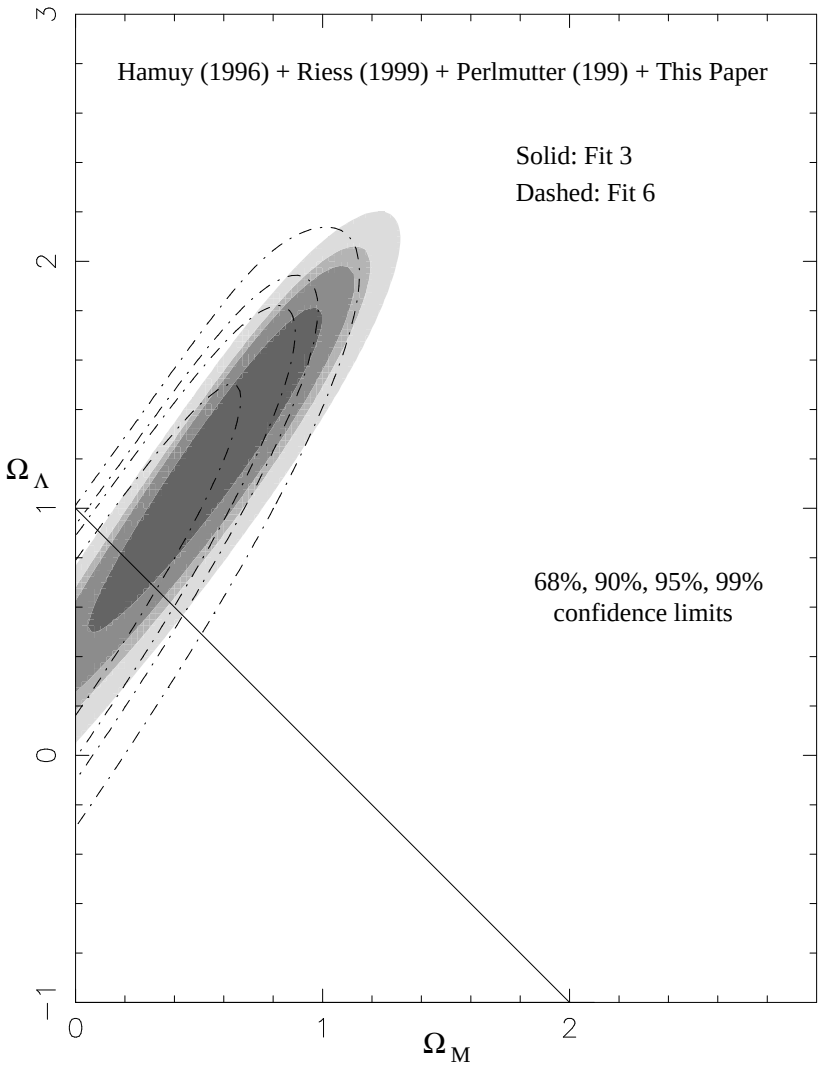

Fig. 7.— Primary confidence intervals on $\Omega_{\rm M}$ and Ω_Λ resulting from this paper. Both sets of contours include all low-z data used in this paper, plus all of the current SCP high-redshift supernovae data, including supernovae from P99 and the WFPC2 supernovae observed in this paper. The filled confidence regions are from Fit 3, which omit supernovae likely to be reddened (E(B-V)$> 3\sigma$). The dashed lines are confidence regions where E(B-V) host galaxy extinction corrections have been directly applied.

dence regions from the three methods overlap. This is a powerful confirmation that we have indeed made meaningful measurements about Cosmology. Any hypothetical systematic which made the supernova results consistent with $(\Omega_{\rm M}, \Omega_\Lambda) = (1, 0)$, for example, would then make those results inconsistent with the intersection of the cluster and the CMB results. The convergence of the three completely independent cosmological measurements provides convincing evidence that a substantial fraction of the energy density of the universe must not be normal matter, i.e. a cosmological constant or dark energy.

The latest SDSS results suggest that if the amplitude of the mass fluctuations on an 8 h^{-1} Mpc scale, σ_8, has a value $\sigma_8 = 1$, then the mass density of the universe is $\Omega_{\rm M} \sim 0.2$ (Bahcall *et al.* 2003). This is lower than the $\Omega_{\rm M} = 0.3$ which is frequently assumed ; $\Omega_{\rm M} = 0.28$ was the maximum likelihood value for a flat universe from P99. The supernovae in this paper also prefer a lower mass density of (Table 8), although $\Omega_{\rm M} = 0.3$ is still consistent to the $\sim 1\sigma$ level. In particular, the fit which includes only the high-redshift supernovae from this paper (Fit 2) has a preferred value $\Omega_{\rm M} = 0.20^{+0.08}_{-0.06}$. With host galaxy E(B-V) corrections applied, that number drops to $\Omega_{\rm M} = 0.12^{+0.10}-0.08$. Fit 6, which includes both these high redshift supernovae and those from P99, and also applies host galaxy E(B-V) corrections, has a flat-universe value of $\Omega_{\rm M} = 0.19^{+0.11}_{-0.07}$.

Putting these new supernova results and the SDSS cluster results together with the evidence for a flat universe from the CMB, a better "consensus cosmology" might be $(\Omega_{\rm M}, \Omega_\Lambda) = (0.2, 0.8)$.

4.1. Dark Energy Equation of State

The fits of the previous section used a traditional Robertson-Walker cosmology where $\Omega_{\rm M}$ was the energy density of cold matter (i.e. pressure $p = 0$), and $\Omega_{\rm M}$ was the energy density in a cosmological constant (i.e. pressure $p = -\rho$, where ρ is the energy density). In Einstein's field equations, the gravitational effect enters in terms of $\rho + 3p$. If $w \equiv p/\rho$ is the equation of state parameter, then for matter, $w = 0$ and for vacuum energy (i.e. a cosmological constant), $w = -1$. In fact, it is possible to achieve an accelerating universe so long as there is a component with $w < -1/3$. The Hubble diagram for high-redshift supernovae provide limits on the value of w (P99). Figure 8 shows the limits on w from the data in this paper. These plots show the joint confidence limits on $\Omega_{\rm M}$ and w, under the assumption (motivated by the CMB results) that the universe is flat, i.e. $\Omega_{\rm M} + \Omega_w = 1$ (where Ω_w is the energy density in the component with equation of state w, in units of the critical density, analogous to Ω_Λ).

The lower panel on each plot applies an additional prior that $\Omega_{\rm M} = 0.19^{+0.08}_{-0.07}$ from the SDSS cluster results (Bahcall *et al.* 2003). Putting the supernova and cluster results together provide the best flat-universe limit we currently have on w. Both with and without host galaxy extinction, with this mass prior w is limited to < -0.7; with host galaxy extinctions applied, that 1σ limit becomes more stringent, $w < -0.8$. However, w is not well bounded from below, and the current data is consistent with values as low as $w = -1.9$ (for Figure 8f, with host galaxy E(B-V) corrections applied). All of the

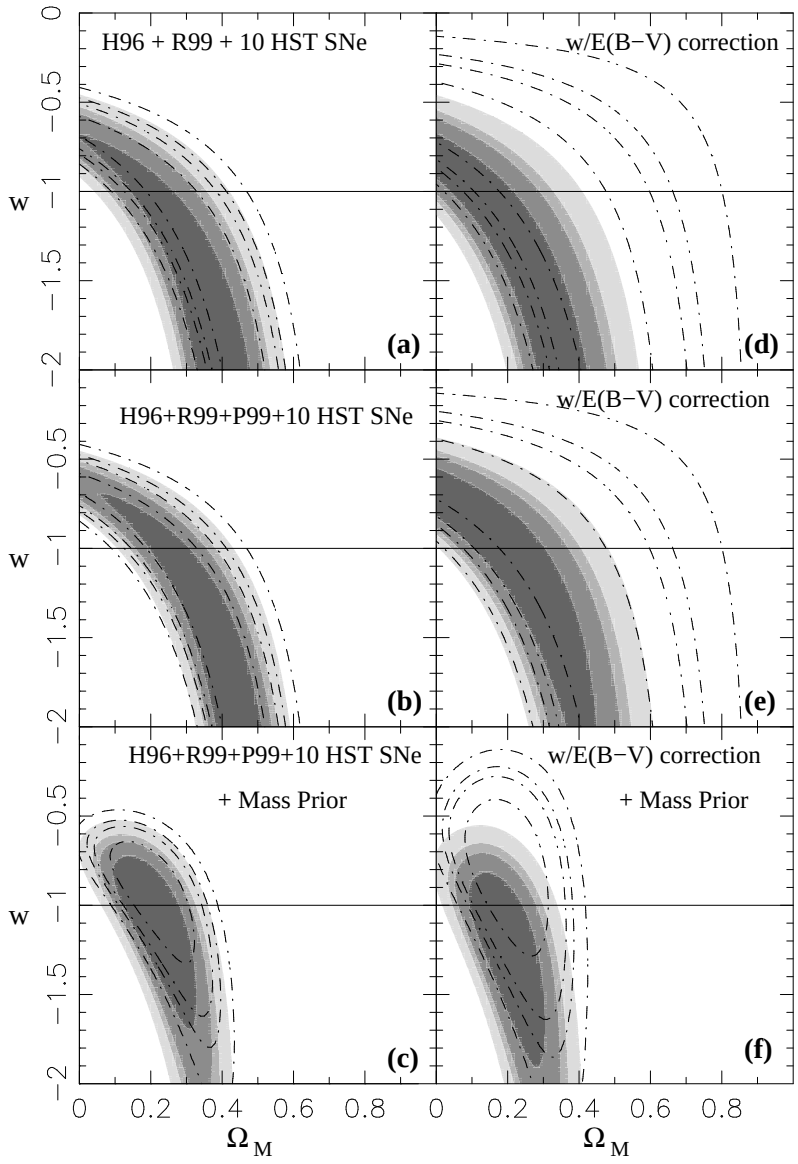

Fig. 8.— Joint confidence limits on $\Omega_{\rm M}$ and w assuming $\Omega_{\rm M} + \Omega_w = 1$. Confidence limits plotted are 68%, 90%, 95%, and 99%. Left panels (a-c): in dashed lines is Fit 1, including only the high-z supernovae from P99, for comparison. No host galaxy E(B-V) corrections have been applied, except to omit significantly reddened supernovae. Solid confidence regions are Fit 2 (only new high-redshift SNe) in (a) and Fit 3 (all high-redshift SNe) in (b) and (c). Panel (c) includes a mass prior $\Omega_{\rm M} = 0.19^{+0.08}_{-0.07}$. Right panels (d-f): in dashed lines is Fit 4 (only P99 high-z SNe). Host galaxy E(B-V) corrections have been explicitly applied here. Panel (d) is Fit 5 (only new high-z SNe), and panel (e) is Fit 6 (all SNe). Panel (f) is (e) with the same mass prior applied.

results are entirely consistent with a low mass ($\Omega_{\rm M} = 0.2$) flat universe dominated by vacuum energy ($w = -1$).

5. Summary and Conclusions

1. We have presented a new, independent set of 11 high-redshift supernovae ($z = 0.36$–0.86). These supernovae have very high-quality photometry measured with WFPC-2 on the HST. The higher quality lightcurve measurements have small enough errors on each E(B-V) measurement to allow direct *individual* correction of E(B-V) host galaxy reddening.

2. We have performed improved color and K-corrections, necessary to combine WFPC-2 photometric filters with ground-based photometric filters. A reanalysis of the P99 supernova lightcurve data with these new corrections shows that the cosmological results of P99 are not significantly changed.

3. The cosmological fits to $\Omega_{\rm M}$ and Ω_Λ are consistent with the SCP's previous results (P99), providing evidence for a cosmological constant to very high confidence. This is a significant confirmation of the results of P99 and Riess (1998), and is the first new complete set of high-redshift supernovae to yield those same results.

4. Under the assumption of a flat universe, all the SNe together yield $\Omega_{\rm M} = 0.24^{+0.07}_{-0.06}$ (where host galaxy extinction is handled by omitting severely reddened supernovae) or $\Omega_{\rm M} = 0.19^{+0.11}_{-0.07}$ (where E(B-V) corrections are applied individually to each SN). Our best joint limits on $\Omega_{\rm M}$ and Ω_Λ, including all the high-redshift supernovae, are shown in Figure 7.

5. The data provide a $1-\sigma$ upper limit on w, the equation of state of the dark energy, of $w < -0.8$, under the assumption of a flat universe (motivated by the CMB) and using the SDSS cluster result of $\Omega_{\rm M} = 0.19^{+0.08}_{-0.07}$ (Bahcall *et al.* 2003).

REFERENCES

Aldering, G., Knop, R., and Nugent, P., 2000, AJ, 119, 2110

Bahcall, N. A., Ostriker, J. P., Perlmutter, S., and Steinhardt, P. J., 1999, Science, 284, 1481

Bahcall, N. A., *et al.*, 2003, ApJ, in press

Branch *et al.*, 1996, in Canal *et al.*, eds., 1996, *Proceedings of the NATO Advanced Study Institute on Thermonuclear Supernovae*

Bessell, M. S., 1990, PASP, 102, 1181

Dolphin, 2000, PASP, 112, 1397

Hamuy, M., *et al.*, 1992, AJ, 102, 208

Hamuy, M., *et al.*, 1996, AJ, 112, 2408

Fruchter, 2000, private communication

Goldhaber *et al.*, 2001, ApJ, 558, 359

Jaffe, A. H., *et al.*, 2001, Phys. Rev. Lett., 86, 3475

Lira *et al.*, 1998, AJ, 115, 234

Mielke *et al.*, 1996, MNRAS, 281, 263

Nugent P., Kim, A., and Perlmutter, S., 2002, PASP, 114, 803

O'Donnell, J. E., 1994, ApJ, 422, 158

Perlmutter *et al.*1999, ApJ, 517, 586

Phillips, M. M., *et al.*, 1999, AJ, 118, 1766

Richmond *et al.*1995, AJ, 109, 2121

Riess, A. G., *et al.*, 1998, AJ, 116, 1009

Riess, A. G., *et al.*, 1999, AJ, 117, 707

Schlegel, D. J., Finkbeiner, D. P., and Davis, M., 1998, ApJ, 500, 525

Suntzeff *et al.*, 1999, AJ, 117, 178

Wells *et al.*1994, AJ, 108,2233

Wu *et al.*, 1995, A&A, 294, L9

This 2-column preprint was prepared with the AAS LaTeX macros v5.0.